Int. J. Electrochem. Sci., 15 **(2020)** 3196 – 3203, doi: 10.20964/2020.04.14

International Journal of
ELECTROCHEMICAL
SCIENCE
www.electrochemsci.org

Short Communication

Formation of hard carbon derived from sulfonated pitch as advanced electrodes for lithium-ion batteries

Jialu Zuo, Yan Guo[*]

College of Chemistry and Chemical Engineering, Inner Mongolia University, Hohhot 010021, P. R. China
[*]E-mail: guoyan@imu.edu.cn (Y. Guo)

Received: 3 December 2019 / *Accepted:* 18 January 2020 / *Published:* 10 March 2020

The exploration for low-cost and sustainable anode materials plays a key role in the future of lithium-ion batteries (LIBs). Sulfonated pitch-based hard carbon obtained by using high-temperature calcination of industrial sulfonated pitch as a raw material is evaluated as an anode material for LIBs. Experimental results show that sulfonated pitch-based hard carbon exhibits excellent electrochemical performance as an anode for LIBs. After 50 cycles, the discharge capacity is still at 310 mAh g^{-1} with a capacity retention rate of 83.8% under a current density of 0.1C. The low-cost and facile synthesis process of sulfonated pitch-based hard carbon makes it a promising anode material for LIBs in the future.

Keywords: lithium ion batteries, hard carbon, sulfonated pitch

1. INTRODUCTION

Lithium-ion batteries (LIBs) are widely used in various electronic devices due to their high energy and power density. The performance of LIBs is closely related to the anode material.[1] Materials made form carbon are typical LIB anode materials that can be further divided into graphite and non-graphite carbon materials. Graphite carbon materials include natural graphite, artificial graphite, and graphitized carbon, while non-graphite carbon materials can be divided into hard carbon and soft carbon.[2-4] Graphite carbon shows good capacity at low pressure, excellent cycling performance, and high coulombic efficiency. Therefore, graphite is the most widely used commercial anode material in lithium-ion batteries.[5-7] However, due to the poor compatibility between graphite and an organic electrolyte, organic solvent molecules easily intercalate into the graphite layer together with lithium ions from the positive electrode during battery cycling; the organic solvent molecules hinder the normal transport of lithium ions, thereby affecting the cycling performance of the battery.[3]

With the advancement and development of science and technology, people require batteries with a high energy density. The theoretical capacity of graphite is only 372 mAh g^{-1}, which greatly limits its development.[8-11] Therefore, the development of high-capacity anode materials has become a key to the development of lithium batteries. Soft carbon is a kind of negative electrode material obtained by low-temperature carbonization.[12] The layered structure of soft carbon is very orderly, and thus, it has a low graphitization, small grain size, large interplanar spacing, and good compatibility with electrolytes. When soft carbon is used as the anode material, it has the advantages of long cycling life, high safety and high temperature charge and discharge capability; however, the irreversible capacity from the first charge and discharge is high, and the output voltage is low.[11, 13]

Hard carbon, which is difficult to graphitize, is generally a pyrolytic carbon obtained by pyrolyzing a polymer, biomass, or the like.[14-17] Since the microstructure of the hard carbon material exhibits a disordered amorphous structure, it can provide more active sites for Li^+ storage, so its theoretical lithium insertion capacity as an anode material for LIBs is approximately twice that of graphite anode materials.[18] In addition, the amorphous structure of hard carbon provides a wide channel for the diffusion and transport of Li^+ inside the material, enabling Li^+ to be inserted and removed more efficiently, which greatly improves the charge and discharge performance of the material under a high current. The unique microstructure of hard carbon promotes excellent electrochemical performance as an anode material for lithium-ion batteries.[19] Compared with traditional graphite anode materials, hard carbon has the advantages of high lithium insertion capacity and good rate performance.[12, 20, 21]

Sulfonated pitch is a modified polymer compound obtained by complex chemical treatment of hydrocarbon-based petroleum compounds through sulfuric acid and other materials, and its main group is sodium sulfonate. Sulfonated pitch is a raw material from commercial industry with a wide range of sources, and thus, it has a low cost. Compared with other carbonaceous precursors, sulfonated pitch can be easily obtained by a simple pyrolysis process. Herein, we highlight a facile calcination strategy to synthesize hard carbon by utilizing sulfonated pitch as the precursor. The as-prepared hard carbon can deliver a high reversible specific capacity and excellent cycling stability, which makes it a promising anode for LIBs.

2. EXPERIMENTAL SECTION

2.1. Material preparation

Sulfonated pitch (Originchem Co., Ltd) based hard carbon was synthesized by a one-step pyrolysis of sulfonated pitch. First, salts and ashes in the sulfonated pitch were thoroughly removed. In this process, 20 g sulfonated pitch was dissolved into 500 ml distilled water and stirred at 80 °C for 4 h. The solution was collected by centrifugation, followed by the addition of 30 ml of concentrated hydrochloric acid for 12 h. Then, the obtained precipitate was washed three times with 1 mol L^{-1} HCl and dried at 80 °C for 12 h to obtain the refined sulfonated pitch. Finally, the refined sulfonated pitch

was transferred into a tube furnace and carbonized at 800 °C for 2 h under nitrogen protection at a heating rate of 2 °C min^{-1}. The obtained hard carbon sample was named HC.

2.2. Characterization

The structures and morphologies of the products were identified by X-ray diffraction (XRD, PANalytical B.V.), X-ray photoelectron spectroscopy (XPS, VG Scientific ESCALAB Mark II spectrometer with a monochromatic A1 Ka X-ray source), and transmission electron microscopy (TEM, FEI Tecnai F20). Structural characterization of the product was performed by Raman spectroscopy using a Renishaw inVia instrument.

2.3. Electrochemical measurements

A working electrode was prepared by mixing the active material, acetylene black and PTFE in a mass ratio of 8:1:1, which was then coated on a Cu foil and dried at 120 °C for 12 h. A lithium sheet was used as the counter electrode and reference electrode. These two electrodes were separated by a Celgard 2400 polypropylene film, and 1 M $LiPF_6$ (EC:DEC = 1:1, mass ratio) was used as the electrolyte. The 2430-type button cells were assembled in an argon-filled glove box. Cyclic voltammetry (CV) tests of the battery were conducted by using a CHl660E electrochemical workstation. Galvanostatic charge-discharge tests were conducted on a Land Battery Tester (Wuhan, China).

3. RESULTS AND DISCUSSION

The crystal information of the HC was obtained by XRD, as shown in Figure 1a. Two relatively broad diffraction peaks are detected at approximately 23° and 43°, corresponding to the (002) and (100) diffraction modes of the graphitic structure, respectively.[22] Thus, it shows the characteristics of disordered carbon materials. Information on the chemical state of the HC surface elements were obtained from the XPS survey spectrum. In the XPS survey spectrum (Figure. 1b), there are two distinct peaks at ~285 eV (C_{1s}) and ~532 eV (O_{1s}), indicating that C and O are the major elements in HC.[23] The C_{1s} and O_{1s} spectra of the HC were deconvoluted to determine the chemical species (Figure 1c and d). The C_{1s} spectrum of the HC in Figure 1c shows three types of carbon, which are C-C (285.1 eV), C-O (286 eV) and O-C=O (289.1 eV). The O_{1s} spectrum (Figure 1d) shows three peaks at binding energies of 531.9, 532.9 and 533.7 eV, which correspond to the C=O bond, C-O bond and O-C=O bond, respectively.[19]

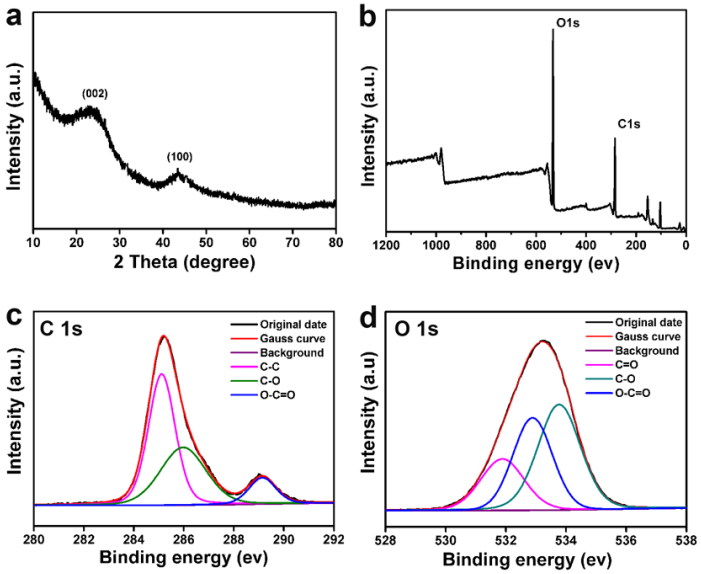

Figure 1. (a) XRD spectrum, (b) XPS survey spectrum, (c) High-resolution XPS scan of the C_{1s}, and (d) High-resolution XPS scan of the O_{1s} for HC.

Figure 2 is the Raman spectrum of HC. It shows two peaks at approximately 1350 cm^{-1} and 1584 cm^{-1}, which correspond to the D-band and the G-band, respectively[24]. The D peak is related to the presence of defects and the G peak is related to graphite crystallinity[25]. In general, the relative intensity of the D-band to that of the G-band (I_D/I_G) indicates the degree of disorder in the graphite structure[14].

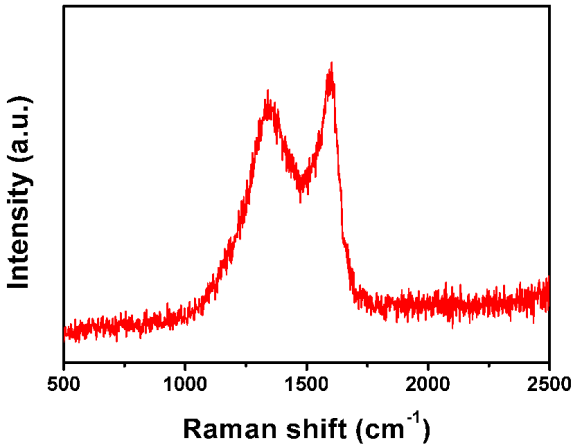

Figure 2. The Raman spectrum of HC.

Figure 3 shows the TEM images of HC to further study the microstructure. There are some local ordered structures owing to the arrangement of graphene sheets under high-temperature calcination. In addition, the sample was observed to be long-range disordered, which is the typical feature of hard carbon, further verifying the amorphous nature of the sample. Moreover, some nanovoids could also be observed in the sample, which are available for lithium ion storage.

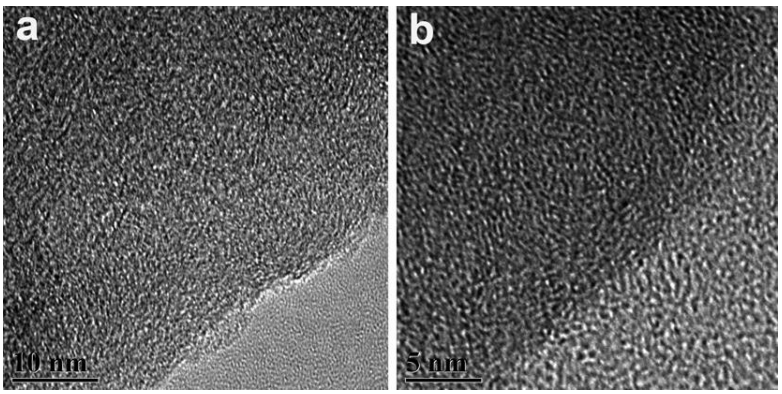

Figure 3. TEM characterizations of HC.

The electrochemical performance of HC as an LIB anode was investigated by using coin-type cells. Figure 4a shows the CV curves of the HC at a scan rate of 0.2 mV s^{-1} over a voltage range of 0-2 V. It can be seen from Figure 4a that the first and second cycle curves do not coincide, corresponding to irreversible capacity. In this process, a reduction reaction occurs at the interface between the electrolyte and the electrode material to form a solid electrolyte interface (SEI), thereby consuming some lithium ions. The second and third cycle curves substantially coincide, indicating good electrochemical stability. The reduction peak at approximately 0.1 V in the first cycle corresponds to the first insertion of lithium ions into the hard carbon material, and the oxidation peak at approximately 0.2 V corresponds to the outflow of lithium ions from the hard carbon.

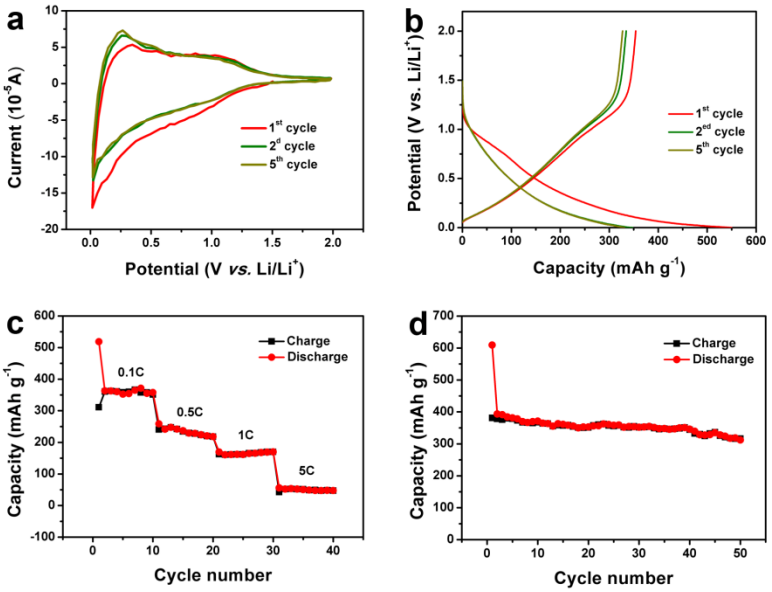

Figure 4. Electrochemical performances of the HC electrode. (a) CV curves at a scan rate of 0.2 mV s^{-1}. (b) Discharge-charge voltage profiles for the 1st, 2ed, and 5th cycles at a current density of 0.1 C. (c) Rate performance. (d) Cycle performance at a current density of 0.1 C.

Figure 4b is a charge-discharge voltage distribution of the first, second, and fifth cycles of HC as an anode material for a lithium-ion battery at a current density of 0.1C. It can be seen from Figure

4b that during the first charging process, a less obvious plateau appeared in the 0.7-1.0 V voltage range, and this plateau disappeared during the second charging process. This is mainly due to irreversible capacity. It is worth noting that in the first charge and discharge curve, the discharge capacity of the electrode material is 550 mAh g^{-1}, while the charge capacity is 387 mAh g^{-1}, resulting in an observable irreversible capacity.

Table 1. Comparison of electrochemical performance of various hard carbon for LIBs.

Material	Current density	Cycle number	Specific capacity (mAh g^{-1})	Reference
Hard carbon/graphene	0.08 A g^{-1}	100	284	Mater. Lett. **2015,** *138*, 259-261
Nanoporous hard carbon	0.1 A g^{-1}	100	230	Electrochim. Acta **2016,** *203*, 9-20
Pitch-based hard carbon	0.1 A g^{-1}	100	258.6	J. Solid State Electrochim. **2017,** *21*, 555-562
Pitch modified hard carbons	0.5 C	100	205	Electrochim. Acta **2012,** *74*, 1-7
Lignin-based hard carbon	2 C	200	225	Electrochim. Acta **2015,** *176*, 1352-1357
Sulfonated pitch-based hard carbon	0.1 C	50	310	**This work**

To further investigate the rate performance of the HC electrode, electrochemical performance tests were conducted at different current densities. Figure 4c shows the rate performance of the HC electrode. When the current densities are 0.1, 0.5, 1, and 5C, the discharge capacities of the prepared electrodes are 360, 210, 155, and 55 mAh g^{-1}, respectively. Even at a relatively high current density of 5C, the specific capacity of the electrode is still 50 mAh g^{-1}, thus exhibiting that it has excellent rate performance.

Figure 4d shows the cycling performance of the HC electrode. The discharge specific capacity can reach up to 370 mAh g^{-1} during the second charge and discharge process at a current density of 0.1C. After 50 cycles, the discharge capacity can still be kept at 310 mAh g^{-1}, with a capacity retention rate of 83.8%, which is comparable to many hard carbon based electrode material (Table 1).[26-30] It can be seen from Figure 4d that the initial coulombic efficiency is 60.8% due to the irreversible capacity. However, in the following cycles, all coulombic efficiencies are above 99.5%. In general, HC exhibits good cycling stability as an anode material for lithium-ion batteries.

The outstanding electrochemical performance of the HC anode is mainly attributed to its unique structure. Sulfonated pitch-based hard carbon consists of a large number of staggered microcrystalline graphite layers and an abundant nanovoids and defects. Its structure is a disordered stack of layers, hich greatly increases its number of active sites that can interact with lithium. In addition, hard carbon has a large interlayer spacing, which facilitates the insertion and extraction of lithium ions. In summary, the special structure of hard carbon promotes its excellent electrochemical performance when used as the anode material for lithium ion batteries.

4. CONCLUSIONS

In conclusion, we report a direct pyrolysis strategy for the synthesis of hard carbon by using sulfonated pitch as a precursor. The as-obtained sample exhibits enhanced electrochemical performance when evaluated as an anode for LIBs. Remarkably, the HC electrode exhibits a high capacity of 370 mAh g^{-1} at a current density of 0.1 C. After 50 cycles, the discharge capacity can still be kept at 310 mAh g^{-1} with a capacity retention rate of 83.8%. This paper presents a low-cost and simple synthesis method for producing a high yield of hard carbon that is promising for large-scale use as anode materials in lithium-ion batteries.

ACKNOWLEDGMENTS
Y.G. acknowledges the financial support from the National Natural Science Foundation of China (Grant No. 21701090), the Natural Science Foundation of Inner Mongolia Autonomous Region of China (Grant No. 2017BS0203), and the Program of Higher-level Talents of Inner Mongolia University (Grant No. 21300-5165154).

References

1. X. Lin, X. Du, P.S. Tsui, J.-Q. Huang, H. Tan, B. Zhang, *Electrochim. Acta*, 316 (2019) 60.
2. H.B. Wu, J.S. Chen, X.W. Lou, H.H. Hng, *Nanoscale*, 3 (2011) 4082.
3. S.L. Candelaria, Y. Shao, W. Zhou, X. Li, J. Xiao, J.-G. Zhang, Y. Wang, J. Liu, J. Li, G. Cao, *Nano Energy*, 1 (2012) 195.
4. L.S. Roselin, R.S. Juang, C.T. Hsieh, S. Sagadevan, A. Umar, R. Selvin, H.H. Hegazy, *Mater.* (Basel), 12 (2019).
5. H. Fujimoto, A. Mabuchi, K. Tokumitsu, N. Chinnasamy, T. Kasuh, *J. Power Sources*, 196 (2011) 1365.
6. X. Li, J. Liu, Y. Zhang, Y. Li, H. Liu, X. Meng, J. Yang, D. Geng, D. Wang, R. Li, X. Sun, *J. Power Sources*, 197 (2012) 238.
7. M. Schroeder, M. Winter, S. Passerini, A. Balducci, *J. Power Sources*, 238 (2013) 388.
8. B. Xu, J. Zhang, Y. Gu, Z. Zhang, W. Al Abdulla, N.A. Kumar, X.S. Zhao, *Electrochim. Acta*, 212 (2016) 473.
9. M. Liu, X. Ma, L. Gan, Z. Xu, D. Zhu, L. Chen, *J. Mater. Chem. A*, 2 (2014) 17107.
10. Y.-J. Han, J. Kim, J.-S. Yeo, J.C. An, I.-P. Hong, K. Nakabayashi, J. Miyawaki, J.-D. Jung, S.-H. Yoon, *Carbon*, 94 (2015) 432.
11. X.-Y. Zhao, X. Bai, W. Yang, D. Shen, H. Yang, N. Lun, Y.-X. Qi, Y.-J. Bai, *New J. Chem.*, 40 (2016) 9986.
12. A. Concheso, R. Santamaría, M. Granda, R. Menéndez, J.M. Jiménez-Mateos, R. Alcántara, P. Lavela, J.L. Tirado, *Electrochim. Acta*, 50 (2005) 1225.
13. F. Bonino, S. Brutti, M. Piana, S. Natale, B. Scrosati, L. Gherghel, K. Müllen, *Electrochim. Acta*, 51 (2006) 3407.
14. A.A. Arie, B. Tekin, E. Demir, R. Demir-Cakan, *Mater. Technology*, 34 (2019) 515.
15. S. Alvin, D. Yoon, C. Chandra, R.F. Susanti, W. Chang, C. Ryu, J. Kim, *J. Power Sources*, 430 (2019) 157.
16. A. Beda, P.-L. Taberna, P. Simon, C. Matei Ghimbeu, *Carbon*, 139 (2018) 248.
17. S.M. Jafari, M. Khosravi, M. Mollazadeh, *Electrochim. Acta*, 203 (2016) 9.
18. H. Yu, X. Dong, Y. Pang, Y. Wang, Y. Xia, *Electrochim. Acta*, 228 (2017) 251.
19. L. Suo, J. Zhu, X. Shen, Y. Wang, X. Han, Z. Chen, Y. Li, Y. Liu, D. Wang, Y. Ma, *Carbon*, 151

(2019) 1.
20. X. Zhang, S. Han, C. Fan, L. Li, W. Zhang, *Mater. Lett.*, 138 (2015) 259.
21. H. Fujimoto, K. Tokumitsu, A. Mabuchi, N. Chinnasamy, T. Kasuh, *J. Power Sources*, 195 (2010) 7452.
22. S.-D. Xu, Y. Zhao, S. Liu, X. Ren, L. Chen, W. Shi, X. Wang, D. Zhang, *J. Mater. Sci.*, 53 (2018) 12334.
23. Y. Zhu, M. Chen, Q. Li, C. Yuan, C. Wang, *Carbon*, 123 (2017) 727.
24. P. Wang, L. Fan, L. Yan, Z. Shi, *J. Alloys and Compd*, 775 (2019) 1028.
25. Y. Li, S. Xu, X. Wu, J. Yu, Y. Wang, Y.-S. Hu, H. Li, L. Chen, X. Huang, *J. Mater. Chem. A*, 3 (2015) 71.
26. X. Zhang, S. Hann, C. Fan, L. Li, W. Zhang, *Mater. Lett.*, 138 (2015) 259.
27. P.-Y. Zhao, J.-J. Tang, C.-Y. Wang, *J. Solid State Electrochem.*, 21 (2016) 555.
28. J. Wang, J.-L. Liu, Y.-G. Wang, C.-X. Wang, Y.-Y. Xia, *Electrochim. Acta*, 74 (2012) 1.
29. S.M. Jafari, M. Khosravi, M. Mollazadeh, *Electrochim. Acta*, 203 (2016) 9.
30. Z.-z. Chang, B.-j. Yu, C.-y. Wang, *Electrochim. Acta*, 176 (2015) 1352.